A Systems Interpretation for Observations of Bird V-formations

P. Seiler, A. Pant, and J.K. Hedrick
Email: {pseiler, pant, khedrick}@vehicle.me.berkeley.edu
Department of Mechanical Engineering
University of California, Berkeley *

Abstract

Birds in V formations are frequently observed and two main hypotheses have emerged to explain this particular geometry: (i) it offers aerodynamic advantages and (ii) it is used to improve visual communication. Both explanations require a bird to track its predecessor. However, most V-formations observed in nature are small and the distribution of wing-tip spacings has a large variation. This suggests that tracking the lateral position of the preceding bird is a difficult task. Control theorists, when trying to control platoons of vehicles, also noted that predecessor following is difficult. In this paper, we apply a result from systems theory to explain the observations of bird V-formations. The strength of this result is that it does not rely on the details of the bird flight model. Thus we claim that formation flight is inherently difficult for birds.

1 Introduction

Bird flocks are frequently observed in nature and numerous reasons have been proposed for this behavior. Flocking may simply be a natural social behavior (Emlen, 1952) or it may be driven by the need to avoid, detect, and defend against predators (Vine, 1971). The coordination exhibited in some bird formations suggests additional motivations. For example, traveling birds are frequently seen in linear formations such as the V, J, or echelon. Using the terminology introduced by Heppner (1974), the J and echelon are variants of the V formation where one leg of the formation is shorter or is missing entirely. Two predominant hypotheses exist to explain the frequent observation of linear formations. One hypothesis is that birds gain some aerodynamic advantage when in a linear formation (Lissaman and Shollenberger, 1970). The alternative hypothesis is that visual communication between flock members is improved leading to enhanced navigation capabilities (Gould and Heppner, 1974; Heppner, 1974). We will give a brief review of these two hypotheses.

An aerodynamic advantage is obtained by flying in the upwash produced by other birds in the formation (Lissaman and Shollenberger, 1970; Badgerow and Hainsworth, 1981; Hummel, 1983, 1995). Specifically, a pair of trailing vortices form 1 to 2 wingspans behind a bird (Higdon and Corrsin, 1978; Badgerow and Hainsworth, 1981). Based on a fixed-wing analysis, the distance between these vortices is $\frac{\pi}{4}b$ where b is the wingspan of the bird (Higdon and Corrsin, 1978; Hummel, 1983, 1995) (see Figure 1). Within the trailing vortices is an area of downwash and outside the vortices is an area of upwash. To obtain maximum lift from this upwash, birds should fly with a wingtip spacing (WTS) of $WTS_{opt} = (\frac{\pi}{4} - 1) \times \frac{b}{2}$. $WTS_{opt} < 0$ which implies that the bird wings should overlap to take full advantage of the upwash. The savings are strongly dependent on lateral position, so a trailing bird must accurately track WTS_{opt}. On the other hand, a consequence of Munk's displacement theorem is that the savings are, more or less, independent of the longitudinal position (Lissaman and Shollenberger, 1970; Hummel, 1983). Thus a bird formation can be staggered to distribute the load evenly among its members without affecting the total induced drag

*This work was supported in part by Office of Naval Research (ONR) under the grant N00014-99-10756.

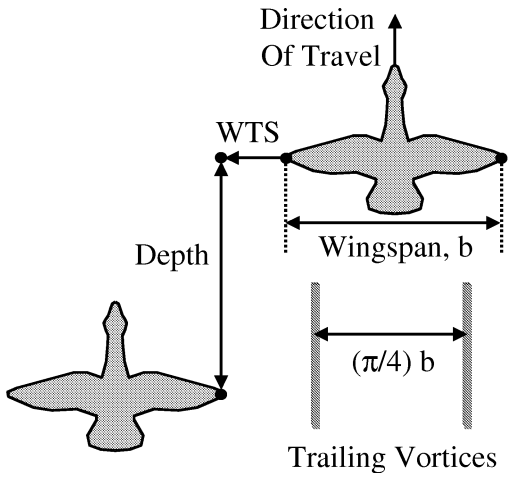

Figure 1: Formation Notation

(Lissaman and Shollenberger, 1970; Hummel, 1983). We should note that these results are based on a fixed wing analysis. As noted in (Badgerow, 1988), the results are likely to be valid for birds with large wing spans and low wingbeat frequency, for example a Canada Goose in steady flight.

The visual communication hypothesis postulates that formation geometry is correlated with retinal features and the location of the eye on the head (Gould and Heppner, 1974; Heppner, 1974; Heppner et al., 1985; Badgerow, 1988). For example, Heppner (1974) speculated that the placement of the eyes restricts the field of vision and this motivates the use of a V formation. The enhanced visual communication may benefit bird flocks in several ways. First, it may aid migratory navigation by averaging the desired directions of all birds (Gould and Heppner, 1974). This ensures the flock saves time and energy by taking the most direct migratory route (Badgerow, 1988). The enhanced visual communication may also increase the probability that flocks are maintained during flight between roosting and foraging areas (O'Malley and Evans, 1982). This would enable group activities to be performed at the destination. Finally, the enhanced visual communication may enable younger birds to learn about migratory paths and/or traditional roosting and feeding areas (Speakman and Banks, 1998).

These two hypotheses lead to different predictions on the relationships between WTS and depth. The aerodynamic advantage hypothesis predicts that WTS will be close to WTS_{opt} with small variance and a positive skew ($WTS \geq WTS_{opt}$). Furthermore, the WTS should be uncorrelated with depth (Badgerow, 1988). The visual communication hypothesis predicts that WTS and depth will be positively correlated to maintain the optimal angle between birds (Badgerow, 1988).

Many researchers have observed and studied bird formations with the goal of testing the predictions generated by these hypotheses (Gould and Heppner, 1974; Williams et al., 1976; Major and Dill, 1978; O'Malley and Evans, 1982; Hainsworth, 1987, 1988; Badgerow, 1988; Cutts and Speakman, 1994; Speakman and Banks, 1998; Weimerskirch et al., 2001). The evidence contained in this body of literature supports the idea that the aerodynamic advantages may be the dominant factor for some birds, such as the Canada Goose (Hainsworth, 1987; Badgerow, 1988), White Pelican (Weimerskirch et al., 2001), and the Greylag Goose (Speakman and Banks, 1998). Badgerow (1988) argued that biomechanical reasons make it particularly important for the Canada Goose to take advantage of the upwash of neighboring birds. On the other hand, observations of the Pink-footed Goose, a smaller bird relatively, favor the visual communication hypothesis (Cutts and Speakman, 1994).

Both hypotheses require a bird to track the lateral position of its predecessor. Two observations in this body of literature imply that this task is difficult for birds in large formations. First, the distribution of wingtip spacings within a formation typically has a large variation. Hainsworth (1987) offers anecdotal

evidence of this variation:

> My observations of flight under windy conditions suggest frequent changes in direction, propagated 'oscillations' along the length of V legs, and a more frequent break-up and reformation of Vs.

Second, the observed formation size is relatively small on average. Hainsworth (1987) noted a further stratification of larger formations into smaller sub-formations.

We hypothesize that the observed behavior is due to an inherent difficulty in tracking the lateral position of the preceding bird. Control theorists made a similar discovery when trying to control platoons of vehicles (Chu, 1974; Hedrick and Swaroop, 1993; Swaroop, 1994; Swaroop and Hedrick, 1996). They noticed that disturbances were amplified as they propagated through a chain of vehicles. Consequently, vehicles in the rear of large platoons oscillated and could not track the preceding vehicle. This effect was termed string instability. In this paper, we use a technical result from systems theory to explain the small formations and poor tracking observed in bird formations.

The remainder of this paper has the following structure: A bird formation model is developed in the next section. In Section 3, we use systems theory to analyze the formation. This analysis provides an explanation for the difficulty of maintaining accurate spacing in large formations. The strength of this result is that it does not rely on the details of the bird flight model described in Section 2. Thus we claim that formation flight is 'inherently' difficult. In Section 4 we discuss the implications of this result and then we offer some conclusions in Section 5.

2 Bird Formation Model

In this section we present a model for a V-formation of birds. The first step is to define the notation for the V formation (Section 2.1). Then we describe the lateral dynamics of an individual bird (Section 2.2). Finally, we present a dynamical model for the lateral motion of an individual bird (Section 2.3).

2.1 Formation Notation

We model each leg of the V formation as a string of $N+1$ birds. Figure 2 displays an abstraction of the first two birds of the V formation. Let $y_0(t)$ denote the Cartesian lateral position of the lead bird and $y_i(t)$ $(1 \leq i \leq N)$ denote the position of the i^{th} follower bird in the string. δ denotes the desired lateral offset between the centers of mass. For example, the optimal wingtip spacing of $WTS_{opt} = (\frac{\pi}{4} - 1) \times \frac{b}{2}$ is equivalent to a desired lateral spacing of $\delta = \frac{b}{8}(\pi + 4)$. As noted in the introduction, birds fly with a large variation about this desired separation. We define their tracking error as $e_i(t) = (y_{i-1}(t) + \delta) - y_i(t)$ for $1 \leq i \leq N$. The goal of the following birds is to force these spacing errors to zero for an aerodynamic advantage or for visual communication.

2.2 Lateral Dynamics

Next we describe the lateral dynamics of an individual bird in the formation. Figure 3 displays these dynamics in a conceptual block diagram. We describe the blocks of this diagram below.

Feedback is used to maintain a desired lateral spacing and this requires the capability to sense the lateral spacing error. Suppose that the bird is flying in formation for an aerodynamic savings. Recall that the aerodynamic savings is strongly dependent on the lateral spacing. Thus a bird will sense a deviation from the optimal wing tip spacing because a larger force will be required for flight. Alternatively, suppose the bird is flying in formation for visual communication. In this case, the placement of the preceding bird in the field of vision can be used to estimate the tracking error. In the remainder of this paper, we assume that a sensed measurement of lateral spacing error with respect to the predecessor is used for control. It is

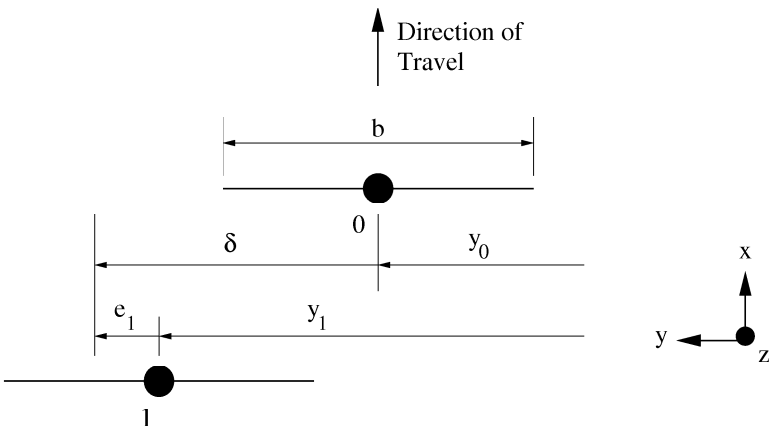

Figure 2: V Formation Coordinates

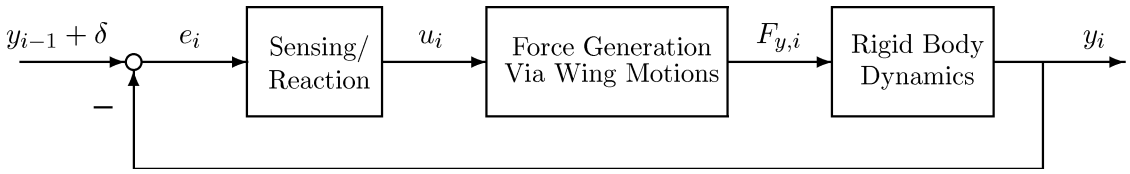

Figure 3: Block Diagram of an Individual Bird

possible that birds in a V-formation triangulate their position with respect to multiple predecessors. The extension of the theory to this scenario remains as future work.

Based on the measurement of e_i, the bird must then change its wing motion to compensate for this deviation. Azuma (1992) described in detail the wing motions of a bird in flight. The force on each wing depends on the complex fluid dynamics generated due to the motion of the wing. For our purposes, it is sufficient to note that based on measurement of e_i, the bird can change its wing motions to generate a total lateral force, denoted $F_{y,i}$.

The final block in Figure 3 consists of the rigid body dynamics of the bird. The lateral motion of the bird that results from $F_{y,i}$ is simply given by Newton's second law. The entire bird model will be described mathematically in the following section.

2.3 Individual Bird Model

To summarize the previous section, the lateral force is generated as a function of the spacing error by a complex dynamical system comprising sensing, reaction, wing motion, and fluid dynamics. Now, for the purposes of analysis, we assume that for small deviations about the nominal formation trajectory, the dynamical system describing the force generation process can be linearized. In other words, we assume the lateral force on the bird can be described by a set of linear, ordinary differential equations:

$$\begin{aligned} \dot{w}_i &= Aw_i + Be_i \\ F_{y,i} &= Cw_i + De_i \end{aligned} \tag{1}$$

where i denotes the i^{th} bird, $w_i \in \Re^n$ is the state, and n is the state dimension. Newton's second law then gives the lateral motion of the bird in terms of this force:

$$m\ddot{y}_i = F_{y,i} \tag{2}$$

Equations 1 and 2 are the model for the lateral motion of a bird in formation flight. We assume that the formation starts with the initial conditions: $w_i(0) = 0$, $\dot{y}_i(0) = 0$ and $y_i(0) = i\delta$ for all i. In other words, the birds start at the correct lateral position and with no lateral motion.

In the following section we show that it is 'inherently' difficult for each bird to track its predecessor. We use the term 'inherent' because the result is independent of the dynamical system used to represent the force generation process (Equation 1). The result holds for any choice of (A, B, C, D) and only relies on the fact that the lateral dynamics are governed by Newton's second law (Equation 2).

3 Formation Analysis

In this section we derive a relation for the the spacing errors in the formation (Section 3.1). We then give a technical result from systems theory (Section 3.2). We apply this result to analyze the lateral spacing errors along one leg of a V formation (Section 3.3). The conclusion is that tight tracking of the desired lateral position is difficult.

3.1 Formation Spacing Errors

In classical control theory, linear dynamical systems are typically written in the Laplace domain. A short introduction on the Laplace Transform is given in Appendix A. In the Laplace domain, the individual bird model (Equations 1 and 2) is given by:

$$Y_i(s) = \frac{1}{s^2} H(s) E_i(s) + \frac{i\delta}{s} \qquad \text{for } 1 \leq i \leq N \tag{3}$$

where $H(s) = C(sI - A)^{-1}B + D$. For notational simplicity, define $L(s) := \frac{1}{s^2} H(s)$. We make the technical assumption that $H(0) \neq 0$. Intuitively, this assumption ensures that the bird dynamics are stable in the face of constant wind gusts.

Using Equation 3, we can write the spacing errors as:

$$\begin{aligned} E_1(s) &= Y_0(s) - Y_1(s) + \frac{\delta}{s} = Y_0(s) - L(s)E_1(s) \\ E_i(s) &= Y_{i-1}(s) - Y_i(s) + \frac{\delta}{s} = L(s)E_{i-1}(s) - L(s)E_i(s) \qquad \text{for } 2 \leq i \leq N \end{aligned}$$

We can simplify these expressions to obtain the following relations:

$$E_1(s) = S(s)Y_0(s) \tag{4}$$

$$E_i(s) = T(s)E_{i-1}(s) \quad \text{for } 2 \leq i \leq N \tag{5}$$

where $S(s) := \frac{1}{1+L(s)}$ and $T(s) := \frac{L(s)}{1+L(s)}$ are known in control theory as the sensitivity and complementary sensitivity functions, respectively. Equation 4 shows that the sensitivity function, $S(s)$, determines the effect of the leader motion, $Y_0(s)$, on the first spacing error, $E_1(s)$. Equation 5 shows that the complementary sensitivity function, $T(s)$, governs the propagation of errors along the leg of the V.

To show that formation flight is inherently difficult, we need some measure of the size of the spacing errors. The following norms measure the size of the corresponding time and Laplace domain functions:

$$\|e_i(t)\|^2 := \int_0^\infty e_i(t)^2 dt$$

$$\|E_i(s)\|^2 := \frac{1}{2\pi} \int_{-\infty}^{\infty} |E_i(j\omega)|^2 d\omega$$

As noted in the appendix, 'size' is preserved when moving between the time domain and Laplace domain: $\|e_i(t)\| = \|E_i(s)\|$. This is known as Parseval's Theorem. It follows from Parseval's Theorem and Equation 4 that if $|S(j\omega)|$ is small for all ω, then $\|e_1(t)\| \ll \|y_0(t)\|$. Similarly, if $|T(j\omega)| < 1$ for all ω, then $\|e_i(t)\| < \|e_{i-1}(t)\|$. Conversely, if $|T(j\omega)| > 1$ for all ω, then $\|e_i(t)\| > \|e_{i-1}(t)\|$.

Unfortunately, since $S(s) + T(s) = \frac{1}{1+L(s)} + \frac{L(s)}{1+L(s)} \equiv 1$, $|S(j\omega)|$ and $|T(j\omega)|$ cannot both be small at any given frequency. Moreover, $T(0) = 1$ and thus it is not possible to have $|T(j\omega)| < 1$ at all frequencies. In fact, the result in the next section implies that the situation is even worse: there is an interval of frequencies such that $|T(j\omega)| > 1$. In words, there is an interval of frequencies where error amplification occurs.

3.2 Main Result

The next theorem implies that there is a frequency interval such that error amplification occurs. This theorem is a result by Middleton and Goodwin (1990) (Looze and Freudenberg, 1996). Similar generalizations to multiple-input, multiple-output systems have been obtained by Chen (Chen, 1998, 2000).

Theorem 1 *Let $H(s)$ be a rational, proper transfer function such that $H(0) \neq 0$. Furthermore, let $L(s) = \frac{1}{s^2}H(s)$ be the open loop transfer function. If the closed loop system is stable, then the complementary sensitivity function, $T(s) = \frac{L(s)}{1+L(s)}$, must satisfy:*

$$\int_{-\infty}^{\infty} \ln |T(j\omega)| \frac{d\omega}{\omega^2} \geq 0 \tag{6}$$

The proof uses results from complex function theory (Middleton and Goodwin, 1990).

We apply this theorem by considering the following sets of frequencies:

$$\begin{aligned} I_1 &= \{\omega \ : \ |T(j\omega)| > 1\} \\ I_2 &= \{\omega \ : \ |T(j\omega)| = 1\} \\ I_3 &= \{\omega \ : \ |T(j\omega)| < 1\} \end{aligned}$$

Since $\log |T(j\omega)| = 0$ if $\omega \in I_2$, Equation 6 can be written as:

$$\int_{I_1} \log |T(j\omega)| \frac{d\omega}{\omega^2} \geq -\int_{I_3} \log |T(j\omega)| \frac{d\omega}{\omega^2} \tag{7}$$

We note that $\log |T(j\omega)| < 0$ if $\omega \in I_3$. Moreover, $|T(j\omega)| \to 0$ as $\omega \to \infty$ and thus I_3 is not an empty set. Consequently, the right side of Equation 7 is strictly positive and hence I_1 is a non-empty set. Continuity implies that there is an interval of frequencies where $|T(j\omega)| > 1$.

Before proceeding, we call attention to the assumption of closed loop stability in Theorem 1. This assumption means that the bird uses an algorithm that allows it to track the predecessor in a 'stable' manner. In other words, the algorithm can be used for predecessor following in a two bird formation. It is the use of this algorithm within a large formation that leads to difficulties. The term 'string instability' has been used in control theory for this phenomenon: a control algorithm which is stable in a classical sense, but leads to disturbance amplification in large formations.

3.3 Analysis of Spacing Errors

In this section, we summarize the result. The spacing errors are related by:

$$E_i(s) = T(s)E_{i-1}(s) \ \text{ for } i = 2, \ldots, N$$

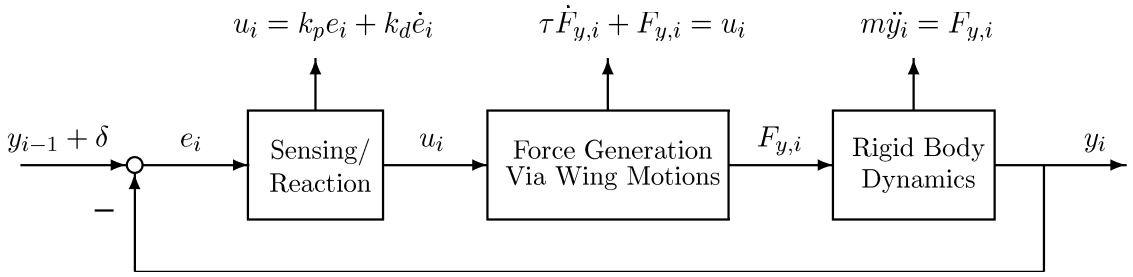

Figure 4: Block Diagram for Simulation

Thus for $i > 1$, $E_i(s) = T^{i-1}(s)E_1(s)$. Furthermore, by the result in the previous section, there is an interval of frequencies such that $|T(j\omega)| > 1$. If the lead bird performs a nontrivial lateral motion, then we can assume, without loss of generality, that $|E_1(j\omega)| \neq 0$ in the given interval. Consequently, $|E_i(j\omega)| \to \infty$ as $i \to \infty$ at these frequencies. The following inequality is less precise, but typically holds: $\|E_i(s)\| > \|E_{i-1}(s)\|$. By Parseval's Theorem, this is equivalent to $\|e_i(t)\| > \|e_{i-1}(t)\|$. In words, it is progressively more difficult for birds which are far from the leader to track the lateral position of the predecessor.

This result is independent of the (A, B, C, D) chosen to represent the force generation dynamics (Equation 1) and relies only on the presence of the rigid body dynamics (Equation 2). We hypothesize that the observed behavior in bird formations is the result of this inherent difficulty in predecessor following.

4 Discussion

In this section, we simulate the lateral dynamics of a flock of birds and interpret the result obtained in the previous section. Figure 4 shows the block diagram corresponding to the simulation model. We assume the bird uses proportional and derivative control to regulate the lateral spacing error to zero. The dynamic equations for this controller are shown above the Sensing/Reaction block. A simple first order lag is used to model the complex force generation dynamics. The rigid body dynamics are as given in Equation 2. Recall that the result in the previous section is independent of the linear dynamics which represent the first two blocks. While the dynamics we have chosen for our simulation are simple, the qualitative results will be unchanged when more complicated models are used.

We simulated one leg of a V-formation with 5 birds. The following numerical parameters were used in the simulation:

$$b = \text{ wing span } = 1.5m \qquad m = \text{ mass } = 2kg$$
$$k_p = \text{ proportional control gain } = 1 \qquad k_d = \text{ derivative control gain } = 2$$
$$\tau = \text{ time constant for wing dynamics } = 0.1sec \qquad \delta = \frac{(4+\pi)b}{8} = 1.33m$$

We note that the parameter values for k_p, k_d and τ have no physiological basis and are chosen for illustrative purposes only. However, the qualitative results predicted by the theory are independent of the values chosen for these parameters. In the simulation, the lateral velocity of the lead bird (i.e. Bird 0) is given by $v_0 = 0.2\sin(0.5t) + 0.05\sin(1.5t)$. The lead bird is moving side-to-side with a small amplitude and the following birds must keep the spacing errors small.

Figure 5 shows the simulation results. The upper subplot shows the spacing errors, $e_i(t)$, as a function of time. As predicted by the previous section, the fourth spacing error has larger oscillations than the first spacing error. This indicates that Bird 4 has a more difficult time tracking its predecessor than Bird 1.

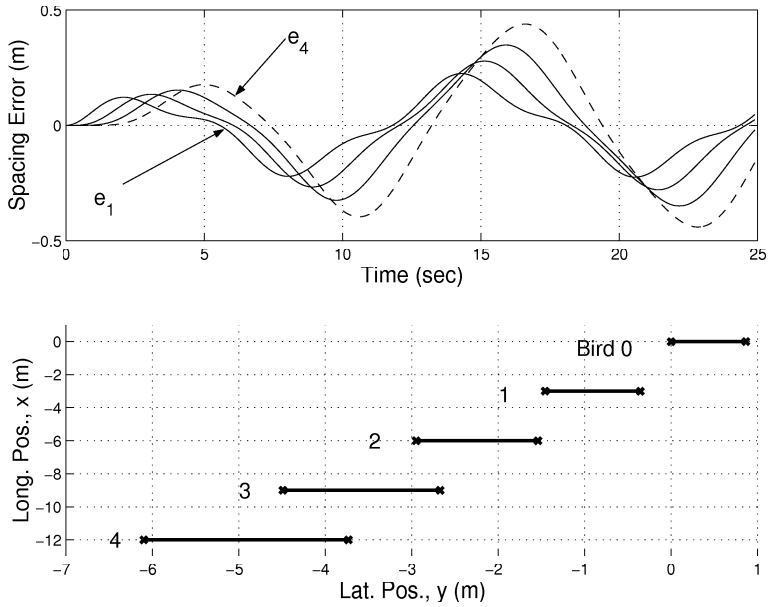

Figure 5: Bird Simulation: Upper subplot shows lateral spacing errors for birds 1 through 4. Spacing errors are larger for birds farther from the leader. Lower subplot shows the range of lateral positions for the leader (bird 0) and all followers. Birds farther from the leader have larger variations in their lateral motions.

The lower subplot shows the range of lateral positions for each bird. The horizontal axis of this subplot is the lateral position with respect to the initial lateral position of Bird 0. The solid lines represent the lateral positions achieved by each bird during the simulation. For example, Bird 0 the moves laterally between 0m and .86m while Bird 4 moves laterally between -6.1m and -3.7m.

Both subplots demonstrate the theoretical result obtained in Section 3: it is inherently difficult for birds to tightly track the lateral position of the preceding bird. This means that birds have a difficult time staying in the optimal position required for visual communication or to obtain the aerodynamic benefits. The simulation results also indicate a method to experimentally test the theory presented in this paper. It has been observed that wing-tip spacings have a large variation. The theory in this paper would be confirmed if it is additionally observed that this variation is larger for birds farther from the leader than for birds closer to the leader. Weimerskirch et al. (2001) has already reported that white pelicans in the rear have particular difficulty maintaining their position. Further data is needed to confirm or disprove the theory proposed in this paper.

5 Conclusions

Most V-formations observed in nature are small and the distribution of wing-tip spacings has a large variation. These observations imply that tracking the lateral position of the preceding bird is a difficult task. In this paper, we used a technical result from systems theory to explain these observations. The strength of this result is that it does not rely on the details of the bird flight model. Thus we claim that formation flight is 'inherently' difficult. The theory in this paper would be confirmed if it is observed that the variation in wing-tip spacing is larger for birds farther from the leader than for birds closer to the leader.

References

Azuma, A., 1992. The Biokinetics of Flying. Springer-Verlag.

Badgerow, J., 1988. An analysis of function in the formation flight of canada geese. Auk 93, 41–52.

Badgerow, J., Hainsworth, F., 1981. Energy savings through formation flight? A re-examination of the Vee formation. J. of Theoretical Biology 93, 41–52.

Chen, J., June 1998. On logarithmic complementary sensitivity integrals for MIMO systems. In: Proceedings of the American Control Conference. pp. 3529–3530.

Chen, J., June 2000. Logarithmic integrals, interpolation bounds, and performance limitations in MIMO feedback systems. IEEE Transactions on Automatic Control 45 (6), 1098–1115.

Chu, K., 1974. Decentralized control of high speed vehicular strings. Transportation Science , 361–384.

Cutts, C., Speakman, J., 1994. Energy savings in formation flight of pink-footed geese. J. of Experimental Biology 189, 251–261.

Emlen, J., 1952. Flocking behavior in birds. Auk 69, 160–170.

Franklin, G., Powell, J., Emami-Naeini, A., 1994. Feedback Control of Dynamic Systems. Addison-Wesley.

Gould, L., Heppner, F., July 1974. The Vee formation of canada geese. Auk 91, 494–506.

Hainsworth, F., 1987. Precision and dynamics of positioning by canada geese flying in formation. J. of Experimental Biology 128, 445–462.

Hainsworth, F., 1988. Induced drag savings from ground effect and formation flight in brown pelicans. J. of Experimental Biology 135, 431–444.

Hedrick, J., Swaroop, D., August 1993. Dynamic coupling in vehicles under automatic control. In: 13th IAVSD Symposium. pp. 209–220.

Heppner, F., 1974. Avian flight formation. Bird Banding 45 (2), 160–169.

Heppner, F., Convissar, J., D.E. Moonan, Jr., Anderson, J., January 1985. Visual angle and formation flight in canada geese {*Branta Canadensis*} . Auk 102, 195–198.

Higdon, J., Corrsin, S., July-August 1978. Induced drag of a bird flock. The American Naturalist 112 (986), 727–744.

Hummel, D., 1983. Aerodynamic aspects of formation flight in birds. J. of Theoretical Biology 104, 321–347.

Hummel, D., 1995. Formation flight as an energy-saving mechanism. Israel J. of Zoology 41, 261–278.

Lissaman, P., Shollenberger, C., May 1970. Formation flight of birds. Science 168, 1003–1005.

Looze, D., Freudenberg, J., 1996. Tradeoffs and limitations in feedback systems. In: Levine, W. (Ed.), The Control Handbook. CRC Press, Ch. 31, pp. 537–549.

Major, P., Dill, L., 1978. The three-dimensional structure of airborne bird flocks. Behavioral Ecology and Sociobiology 4, 111–122.

Middleton, R., Goodwin, G., 1990. Digital Control and Estimation: A Unified Approach. Prentice Hall, Englewood Cliffs, N.J.

O'Malley, J. B. E., Evans, R. M., 1982. Structure and behavior of white pelican formation flocks. Canadian J. of Zoology 60, 1388–1396.

Speakman, J., Banks, D., 1998. The function of flight formations in Grelag Geese *Anser anser*; energy savings or orientation? Ibis 140, 280–287.

Swaroop, D., 1994. String stability of interconnected systems: An application to platooning in automated highway systems. Ph.D. thesis, University of California at Berkeley.

Swaroop, D., Hedrick, J., March 1996. String stability of interconnected systems. IEEE Transactions on Automatic Control 41 (4), 349–356.

Vine, I., 1971. Risk of visual detection and pursuit by a predator and the selective advantage of flocking behaviour. J. of Theoretical Biology 30, 405–422.

Weimerskirch, H., Martin, J., Clerquin, Y., Alexandre, P., Jiraskova, S., October 2001. Energy saving in flight formation. Nature 413, 697–698.

Williams, T., Klonowski, T., Berkeley, P., July 1976. Angle of canada goose V flight formation measured by radar. Auk 93, 554–559.

A The Laplace Transform

In this appendix, we present a brief introduction to the Laplace transform. This tool is commonly used in classical control analysis (Franklin et al., 1994).

In this paper, we assume the lateral force generation process can be modeled by a linear system for small maneuvers around the nominal formation trajectory. A finite dimensional, linear dynamical system can be represented as a collection of first order, ordinary differential equations (ODEs):

$$\begin{aligned} \dot{x} &= Ax + Bu \\ y &= Cx + Du \end{aligned} \tag{8}$$

where $A \in \Re^{n \times n}$, $B \in \Re^{n \times 1}$, $C \in \Re^{1 \times n}$, and $D \in \Re$. $x \in \Re^n$ is the state and n is the state dimension. u and y are the inputs and outputs of the system, respectively. This is referred to as state space form.

Next we define the Laplace transform:

Definition 1 *The* **Laplace Transform** *of a function $f(t)$, denoted $\mathcal{L}\{f(t)\} = F(s)$, is given by:*

$$F(s) = \int_{0^-}^{\infty} f(t) e^{-st} dt$$

Note that $F(s)$ is a function of the complex number s and is defined when the integral converges. The Laplace Transform has several properties which make it useful for the analysis of linear systems. The following property is relevant to this paper:

$$\mathcal{L}\left\{\frac{df}{dt}\right\} = sF(s) - f(0^-)$$

For example, if we assume $x(0) = 0$ and take the Laplace Transform of Equation 8, we obtain:

$$\begin{aligned} sX(s) &= AX(s) + BU(s) \\ Y(s) &= CX(s) + DU(s) \end{aligned}$$

From this equation, we get $Y(s) = \left[C\left(sI - A\right)^{-1} B + D\right]U(s) := H(s)U(s)$. $H(s)$ is called the *transfer function* from u to y. It is simply a rational function of the complex variable, s:

$$H(s) = \frac{a_n s^n + \cdots + a_1 s + a_0}{b_m s^m + \cdots + b_1 s + b_0}$$

We say that $H(s)$ is proper if $m \geq n$.

In the time domain, the input and output of Equation 8 are related by a linear dynamical system. Note that in the Laplace domain, $Y(s)$ is given by simply multiplying $U(s)$ by the transfer function, $H(s)$. Th Laplace domain approach is commonly used in linear systems theory and we enumerate some of its useful properties below.

With some work, it can be shown that if the input $u(t)$ is sinusoidal, i.e. $u(t) = \sin(\omega t)$, then the steady state output of the linear system is given by: $y(t) = |H(j\omega)| \sin(\omega t + \angle H(j\omega))$. For a single sinusoid input, the output is just a scaled and phase shifted version of the input sinusoid. Similarly, suppose the input is a sum of many sinusoids:

$$u(t) = \sum_{k=1}^{N} a_k \sin(\omega_k t)$$

In this case, the steady state output is given by:

$$y(t) = \sum_{k=1}^{N} a_k |H(j\omega_k)| \sin(\omega_k t + \angle H(j\omega_k))$$

This idea can be extended to general inputs that are not just the sum of sinusoids. Thus $H(j\omega)$ represents all of the information about the system response in a concise way.

In addition to the above, it can be shown that transforming time domain signals to Laplace domain preserves 'size'. Specifically, define the norm of a time domain signal as: $\|f(t)\|^2 := \int_0^\infty f(t)^2 dt$. This is, in some sense, a measure of the size of the signal. Let $F(s)$ denote the Laplace Transform of $f(t)$ and define the norm of $F(s)$ as: $\|F(s)\|^2 := \frac{1}{2\pi} \int_{-\infty}^{\infty} |F(j\omega)|^2 d\omega$. Parseval's Theorem says that $\|f(t)\| = \|F(s)\|$. Intuitively, Parseval's Theorem says that the energy of the signal is conserved when we move between the time and Laplace domains.